Journal of Engineering Science and Technology
Special Issue on Development of Sustainability Systems - I, 117 - 130


# NUMERICAL SIMULATION OF A POROUS MEDIA SOLAR COLLECTOR INTEGRATED WITH THERMAL ENERGY STORAGE SYSTEM

MOHAMMED Y. NAWAF[1], ABDULRAZZAK AKROOT[1], HASANAIN A. ABDUL WAHHAB[2, *]

[1]Department of Mechanical Engineering, Faculty of Engineering, Karabuk University, 78050 Karabuk, Turkey
[2]Training and Workshop Centre, University of Technology- Iraq, Baghdad, Iraq
*Corresponding Author: 20085@uotechnology.edu.iq

**Abstract**

Increasing the contact area between the working fluid and solid surface is proven to be a successful technique for enhanced heat transfer. This paper presents computational simulation results of a closed active solar water heating system. The system is a novel solar water heating as it is compacted with a heat transfer unit filled with an open cell foam porous media for increased heat transfer area and molten salts of 60% sodium nitrate and 40% potassium nitrate as phase change material. Water is circulated between the collector and a storage tank. The numerical simulation and analysis were performed using ANSYS FLUENT 17.0, assuming a steady, incompressible, and 3D state. The system performance was tested using two flow rates of the circulating water of 2.5 and 3.5 l/min. Numerical results showed that the temperature difference between the inlet and outlet decreases with increasing water flow rates through the solar water heater. The temperature difference decreased by 11.5% when the flow rate increased from 2.5 to 3.5 l /min. Also, the results showed a good prediction of the real flow behaviour inside the thermal energy storage. Also, the evolution of the numerical simulation accuracy for porous media solar collector analysis is still a topic of future research.

Keywords: open-flow material foam, porous media, solar collector simulation, thermal energy storage.

## 1. Introduction

The energy demand is growing exponentially while the role of the limited resources of fossil fuels becomes apparent, so the use of renewable energies has become an urgent issue in our world today. With a simple comparison between the sources of renewable energies, solar energy takes the lead as the most source that can be used safely due to its availability and spread, as it is frequently used in heating, electricity, and light [1, 2]. The issue of solar radiation concentration plays a major role in designing highly efficient solar systems, especially solar energy collectors, as an essential part, as it is the approved method for collecting solar thermal energy [3-5]. Thermal energy storage units follow this. This second important part enhances the role of the solar energy system, relying on providing energy at times when the solar radiation is gone [5, 6]. In solar heating systems, the system is designed to provide a black absorbent surface to ensure high-quality absorption of solar radiation. Then, these rays are converted into heat that is transferred to a liquid that flows through the system. Recently, porous materials have been used, and solid nanoparticles have been added to conventional fluids to develop these systems by increasing the heat transfer coefficients [7-9]. While many researchers were interested in improving the thermophysical and radiation properties [10, 11].

Many methods have been applied in solar energy collectors, including volumetric absorption collectors, where light is absorbed depending on the volume of the liquid. At the same time, the other type is called flat plate collectors, in which solar radiation is absorbed through its surface [12]. So, the collector cover's temperature will increase, leading to increased thermal losses [13]. On the other hand, volumetric absorption solar collectors have less thermal resistance to converting solar radiation into heat due to the absence of tubes [14]. The optical analysis of the properties of porous foams and nanofluids is an important step in their use as direct adsorbents in volumetric absorption collectors [15, 16]. Porous fillings are usually made of metal or ceramic materials. The fact that ceramics have more advantages over metals, in addition to being resistant to corrosion and able to be used at very high temperatures [17]. Whereas ceramic has a lower thermal conductivity compared to metallic materials. Also, in terms of composition, porous foams have a high porosity coefficient (usually between 75% and 95%) and have an open lattice structure [18-20]. Wang et al. [21] used the Mie technique to calculate the optical properties of the SiC-fabricated porous foam. The study included the effect of pore size on the optical properties. Their data confirmed that a scattering phase function could be assumed for all SiC 0.6 porous foams and considered the extinction coefficient converging on the scattering coefficient.

Menbari et al. [22] relied on the random method of spherical particles to represent porous materials by applying the Rossland extinction coefficient, where they assumed the existence of independent scattering. While the achieved extinction coefficient was dependent on the diameter of the cells as a function of the porous materials. Dissa et al. [23] reported the extinction coefficient of porous SiC foam based on the Monte Carlo basis. The results confirmed that the extinction coefficient highly depends on the porosity ratio and pore size. Where the error percentage of the theoretical results was less than 15% compared to the experimental data. Recently, many researchers have done many research studies on using porous absorbents with variable porosity and pore size. Du et al. [24] investigated the radiometric properties of volumetric absorbents with variable cell porosity. The results proved that reducing the porosity, especially in the inner layers of the material, makes it more absorbent of radiation compared to fixed porosity, and the losses within the radiation form are reduced. Valizade et al. [25] experimentally studied the effect of porosity, pore diameter, and material type on radiative properties. The pore diameter and porosity had a greater effect on the optical properties of porous foams than on material type.

Many studies have been done on improving the performance of the storage unit by reducing the layers of the water tank and the effect of heat loss. Other optimization techniques include optimizing tank design, insulation materials, incorporating a storage tank within the collector, and a heat exchanger immersed or placed outside the tank. Mai et al. [26] studied the thermal performance of a domestic hot water cylindrical tank encapsulated with PCM experimentally and validated the result numerically using the finite volume method. The electrical efficiency available during the night was enough in all cases experienced. Mehling and colleagues. Mehling et al. [27] prepared an experimental and simulated analysis of different cylindrical storage units to analyse the heat capacity and storage density. The system uses a PCM unit on top of the thermal cylindrical tank. Results show that the tank configuration retains warm water for 50% to 200% longer and increases average density by 20% to 45%. Dheep and Sreekumar [28] experimentally studied the performance of a thermal storage tank incorporated with PCMs of sodium thiosulfate pent hydrate using conventional open-loop passive solar water heating. The recorded storage time of hot water produced increased, and total heat accumulated in the SWH system. Also, it was found that hydrated salts of the highest solar thermal energy storage performance in PCM used in the theoretical investigation were disodium hydrogen phosphate dodecahydrate and sodium sulphate dehydrate. Generally, the main objective of the present study is a numerical analysis of solar water heating systems, when solar collectors designed depend on open cell foam porous media with properties (transmittance coefficient, extinction coefficient, and penetration depth) and thermal energy storage unit contains on molten salts are typically made up of 60% sodium nitrate and 40% potassium nitrate. The obtained data are useful in applying porous foam as a direct absorber in solar collectors.

Compacted solar collectors are a new type of integration of TES with collector in one unit. Saw and Al-Kayiem [29] and Al-Kayiem and Lin [30] used Paraffin wax as TES, while Benhouia et al. [31] used sand as TES material. In both works, the water tubes are in direct contact with the TES materials. The studies showed enhanced efficiency of the water heating and elongated performing time of the compacted collectors.

Darwesh et al. [32] used Paraffin wax as PCM inside a metal cylinder immersed in 1.0 $m^3$ water tank and integrated with 10 solar collectors arranged in two rows. Experimental results show that a water-PCM storage tank resulted in electricity savings of 4.75 kWh, with a total system energy savings of 30.2 kWh as the operation time of the auxiliary electric heater was reduced. The overall system efficiency increased by 25%. Agalave et al. [33] experimented the enhancement of compacted FPC with RES and integrated with separated TES using PCM. Meaning that there are two TES zones. The study concluded that the proposed integrated system offers a viable solution for achieving desired fluid heating in diverse applications.

The production of hot water with a conventional flat plate solar collector system combined with an electric heater to substitute for the night period when there is no solar radiation continues to contribute to the emission of greenhouse gases and points to the limitation in solar energy in domestic water heating. To reduce this limitation, by providing an extended working period for the flat plate solar collector system beyond daytime hours only, this present work identifies three distinct problems that could be addressed, which motivate this paper, namely: new design of flat solar collector with porous media, the integration of the collector with thermal energy storage unit, the material of the thermal energy storage and the limitation in traditional working fluids.

## 2. Material and Methodology

The section presents and discusses the research approach in this study, which has adopted a build model and theoretical and simulation analysis to achieve the study's objectives. The material characterization techniques and equipment used are highlighted accordingly in the section. A flat porous media collector (FPMC) integrated with a thermal energy storage (TES) close loop system is designed and developed for the outdoor environment. The numerical model was developed and was divided two operational cases of FPMC and TES. All models used computational simulation by ANSYS software. A simple solar water heater system using solar energy with weather conditions of Baghdad, Iraq is simulated. The schematic of the model description is shown in Fig. 1.

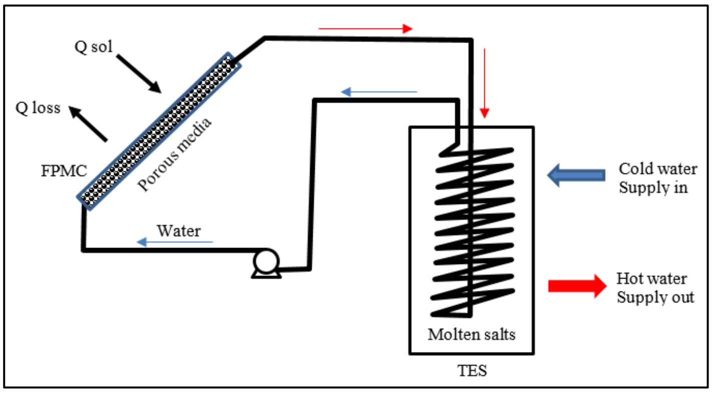


**Fig. 1. A schematic solar domestic water heating application.**

### 2.1. Simulation processes

The numerical analysis processing tools in the commercial CFD software ANSYS 17.2 FLUENT and SolidWorks ver. 2019 (used to model and draw flat porous media collector and thermal energy storage) were used in the current simulation [26]. Several steps have been followed to complete the successful simulation, as depicted in Fig. 2. The creation of the geometric model is the first step in the analysis of the thermal system because it represents the formative basis for the field of modelling, hence the difficulty in analysing complex systems in terms of geometric shape, which are random in construction in terms of shape and dimensions, where open-celled porous materials are considered one of them, as induction adopted it Scientific in many modern engineering applications.

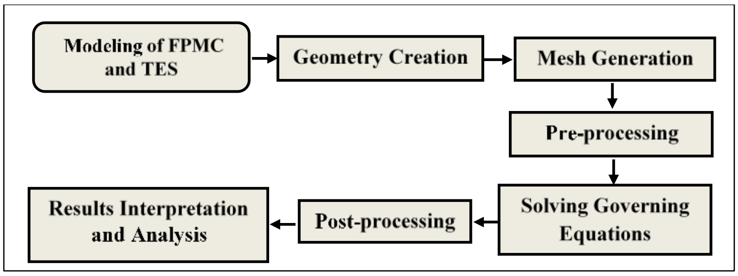


**Fig. 2. Simulation steps in ANSYS 17.2.**

## i. FPMC model

Through geometrical analysis of the cross-section of an open-cell porous material with a porosity of 80%, where 6.3 mm was the most equivalent cell diameter, and the highest frequency, which reached 215 within an area of 100 mm × 100 mm, preparing a computational domain is the first step in CFD simulation. The computational model of the open foam cells was created in SolidWorks 2019 software. The computational model is shown in Fig. 3(a). The element of a small part from porous media is designed of 15 spherical cells at a diameter of 6.3 mm collected as a cubic element. The dimensions of the porous filling are 600 mm width × 390 mm length × 10 mm thickness, made of Aluminium, as shown in Fig. 3(a). A computational fluid dynamics (CFD) model is developed to simulate and investigate the heat transfer from the solar collector to the heating system for used porous media and parameters, such as inlet water temperatures and water flow rates.

## ii. TES model

A fluid-filled thermal storage tank at 500 mm diameter and 1000 mm height with an immersed heat exchanger system includes a helical copper pipe at 16 mm diameter with 17 rolls. The schematic of the subroutine tank is shown in Fig. 3(b). The fluid in the storage tank interacts with fluid in an immersed heat exchanger by heat transfer with the thermal environment via thermal losses.

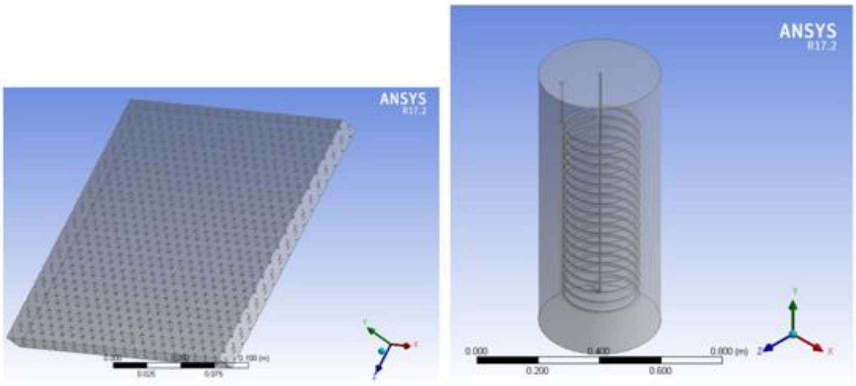


**(a) FPMC model.** **(b) TES model.**

**Fig. 3. Computational domain.**

## 2.2. Mesh generation and mesh independence check

Unstructured meshing is used to mesh the collector domain (The porous filling) with tetrahedral elements. Because of the complex geometry, unstructured tetrahedral meshing was chosen. A mesh-independent solution is recommended to remove the influence of mesh size. When the grid size does not affect the solution, the optimal grid size is chosen. The collector model's 3D meshed geometrical porous filling is shown in Fig. 4(a). The fine meshing scheme produced the most accurate and comparable results for heat transfer inside the flat collector, velocity, and temperature distribution behaviour. As a result, the fine mesh was chosen for the simulations and result interpretation. The computational model had 99458 nodes and 833214 fine mesh elements. While Fig. 4(b) shows the 3D meshed geometrical model of thermal energy storage, this model had 123453 nodes and 911453 fine mesh elements.

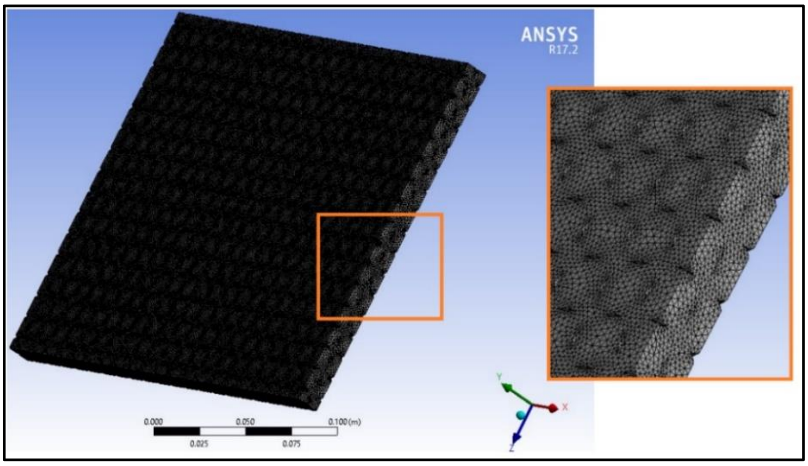


**(a) Mesh of FPMC collector.**

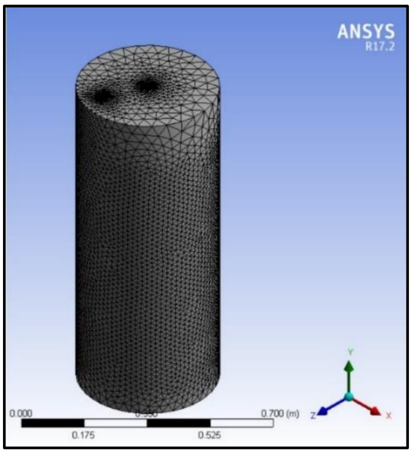


**(b) Mesh of thermal energy storage (TES).**

**Fig. 4. Meshing criteria of the computational domains.**

## 2.3. Governing equations

The governing equations are solved in numerical computational cells. The equations represent the conservation equations,

- Conservation of mass represented by the continuity equation:

$$\frac{\partial}{\partial x}(\rho u) + \frac{\partial}{\partial y}(\rho v) + \frac{\partial}{\partial z}(\rho w) = 0 \tag{1}$$

- Conservation of momentum:

$$\rho \frac{D\vec{V}}{Dt} = \rho \vec{g} - \nabla \vec{\rho} + \frac{1}{3}\mu \nabla (\nabla . \vec{V}) + \mu \nabla^2 \vec{V} \tag{2}$$

- Conservation of energy, as:

$$\frac{\partial}{\partial x_i}[u_i(\rho E + p)] = \frac{\partial}{\partial x_j}\left(k_{eff}\frac{\partial T}{\partial x_j} + u_i(\tau_{ij})_{eff}\right) + S_h \tag{3}$$

The standard *k*-*ε* model has been used to analyse the new cooling system in two important ways: the realizable *k*-*ε* model contains an alternative formulation for the turbulent viscosity and a modified transport equation for the dissipation rate, ε, has been derived from an exact equation for the transport of the mean-square vorticity fluctuation. The turbulence kinetic energy, *k*, and its rate of dissipation, ε, are obtained from the transport equations recommended by [14],

$$(\tau_{ij})_{eff} = \mu_{eff}\left(\frac{\partial u_j}{\partial x_i} + \frac{\partial u_i}{\partial x_j}\right) - \frac{2}{3}\mu_{eff}\frac{\partial u_k}{\partial x_k}\delta_{ij} \tag{4}$$

Where $E$ is the total energy, $k_{eff}$ is the effective thermal conductivity, and $(\tau_{ij})_{eff}$ is the deviatoric stress tensor.

$$k_{eff} = k + \frac{cp\mu_t}{Pr_t} \tag{5}$$

Where *k*, in this case, is thermal conductivity. The default value of the turbulent Prandtl number is 0.85, and the effective thermal conductivity is in the case k-ε model.

$$k_{eff} = \alpha c_p \mu_{eff} \tag{6}$$

The coefficient, α is calculated from $\alpha_o = 1/Pr$

## 2.4. Initial and boundary conditions

The model is used to calculate the solar heating system's values. Input parameters, which are temperature and water mass rate. Table 1 shows the numerical parameters chosen at the heating collector inlet and outlet. The numerical simulation was then performed for the same real conditions. The FPMC numerical simulation was successfully completed, and the results were compared to experimental measurements in the literature. The effects of increasing temperature, water flow rate, and porosity on heating collector and thermal energy storage performance were investigated using significant values of the same parameters. All parameters and variables were fed into the CFD simulation as inputs, and the output parameters were related to temperature distribution, pressure distribution, velocity gradation of tangential and vertical components, and so on.

**Table 1. Simulation parameters.**

| Item | Values | Remarks |
|---|---|---|
| **Water inlet Temperatures** | $T_{w.in}$ = 303 – 314 K | Experiment results of [17] |
| **Ambient Temperatures** | $T_{amb}$ = 303 – 308 K | 12.2 |
| **Solar irradiance** | 29 to 1112 W/m$^2$ | 7.5 |
| **Water density** | 1000 kg/m$^3$ | |
| **Water viscosity** | 1.0016 kg/m·s | |
| **Water flowrate** | 2.5 and 3.5 l/min | |
| **Gravitational acceleration** | -9.81 m/s$^2$ | |
| **Thermal energy storage** | Molten salts | made up of 60% sodium nitrate and 40% potassium nitrate, and the salts melt at approximately 220 °C [29]. |

## 3. Results and Discussion

Figure 5 shows the temperature distribution contours of the FPMC model of the porous media (open foam) water heating collector through different daily times at 2.5 l/min, with the increased water temperature gradually with increasing solar radiation falling on the upper cover of the collector at the same flow rate conditions. The maximum water temperature of the heating system at 12:00 pm was 61.3°C and 58.2°C for water flow rates of 2.5 l/min and 2.5 l/min, respectively. The increase in the water temperature is due to the solar energy absorbed from the upper cover of the collector. This result is close to the experiments of Khafaji et al. [18].

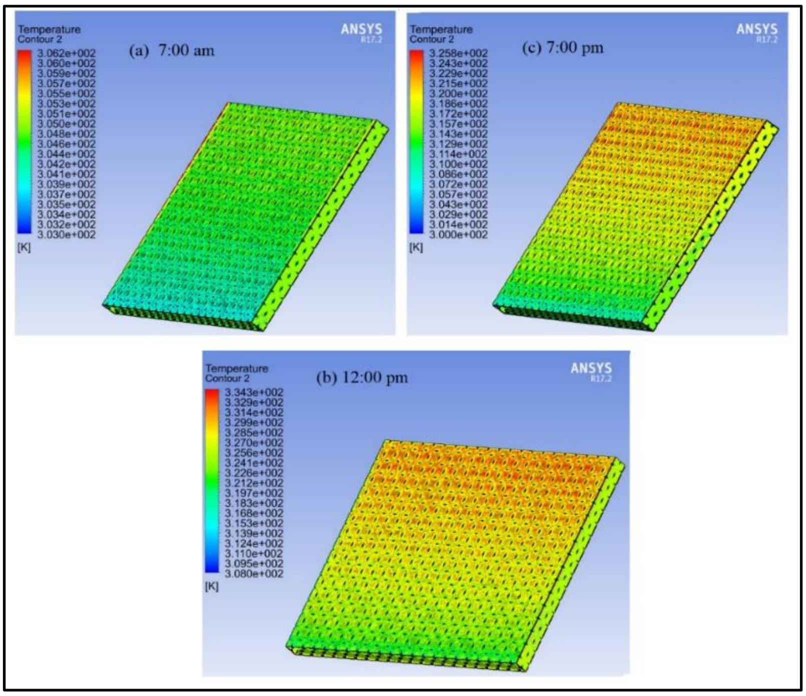


**Fig. 5. Contours of temperature distribution for the FPMC model of the porous media heating collector through different daily time at 2.5 l/min.**

Figure 6 shows the relationship of water temperature difference between inlet and outlet of the heating collector (ΔT) with daily time at different water flow rates. The net addition water heat has been chosen as the comparison parameter at the basic value at a low water flow rate of 2.5 l/min. In detail, the curves show a good agreement with increasing time. Also, the increase in water flow rate reduces ΔT daily. It can be noticed from the numerical results when heating with water and releasing different flow rates that the higher the flow rate, the lower the temperature difference, while the highest difference is at the lowest flow rate. Theoretical results showed that the difference in inlet and outlet temperatures decreases with increasing water flow rates, with the decreasing percentages being 11.5%, when changing the flow rate to 3.5 l/min.

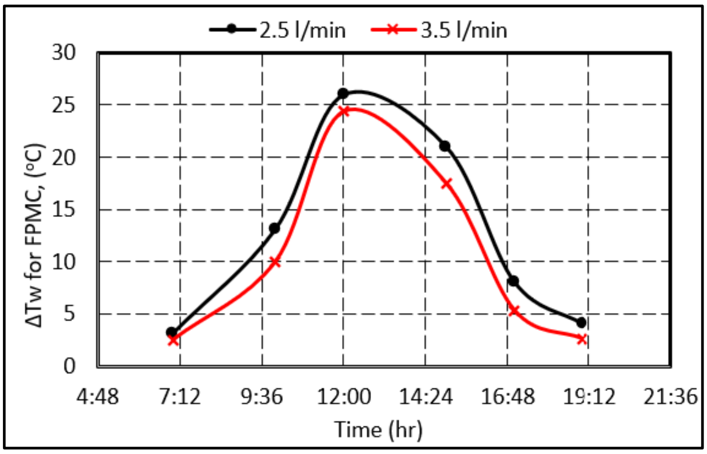


**Fig. 6. Simulated transient behaviour of the water temperature difference between the inlet and outlet for the heating system at different water flow rates.**

As a typical case, a tank that fully absorbed heating material (molten salts are typically made up of 60% sodium nitrate and 40% potassium nitrate) and put in its helical heat sink was chosen to examine the behaviour of the effective thermal conductivity during charge and discharge in the different modes. The represented contours are the radial section in Fig. 7, displaying the spatially variable behaviour from the center to the edge. The figure shows the visible changes in the thermal conductivities over the daytime. Generally, the behaviours of the thermal conductivities of the heating kept changing as the melting progressed, indicating different melting speeds depending on the different tank locations. The thermal conductivities were higher from the edge to the center, indicating the melting speed at the tank center was faster than the tank edge. We can see that the proposed effective thermal conductivity model properly includes this different melting speed depending on the heat sink location in the tank.

Figure 8 shows the relationship of the water temperature difference between the inlet and outlet of the fully absorbed heating material tank with daily time at different water flow rates. The net reduction of water heat to molten salts (typically 60% sodium nitrate and 40% potassium nitrate) has been chosen as the comparison parameter at the basic value at a low water flow rate of 2.5 l/min. In detail, the curves show a good agreement with increasing time. Also, the increase of water flow rate reduces ΔT during a daily time.

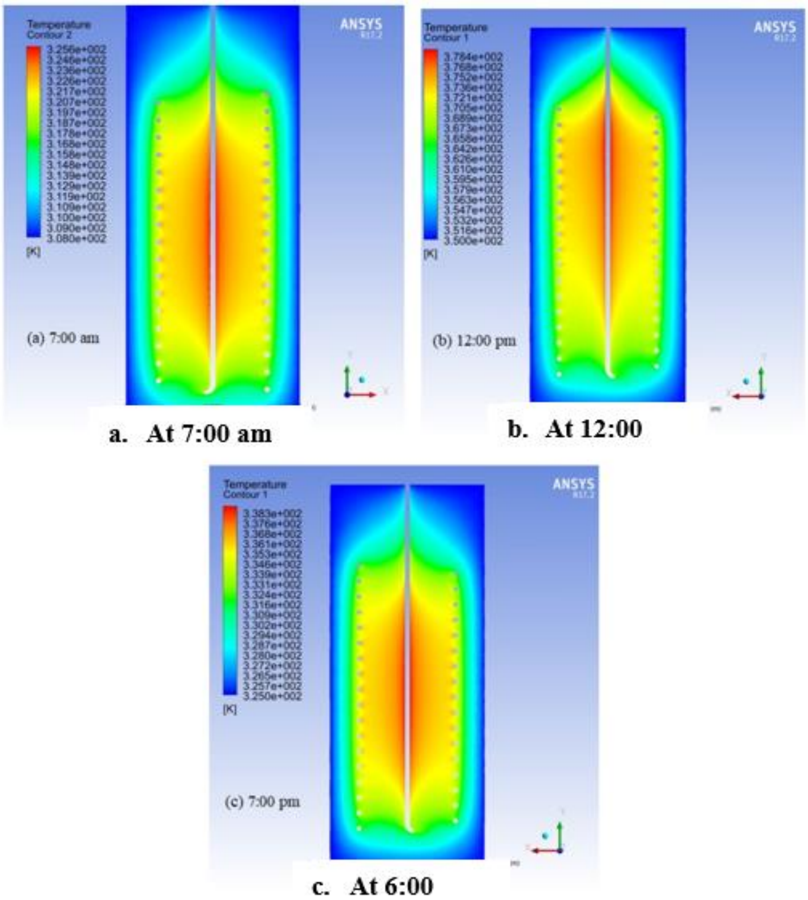


**Fig. 7. Contour of temperature distribution for the TES model of the fully absorbed heating material tank through different daily times at 2.5 l/min.**

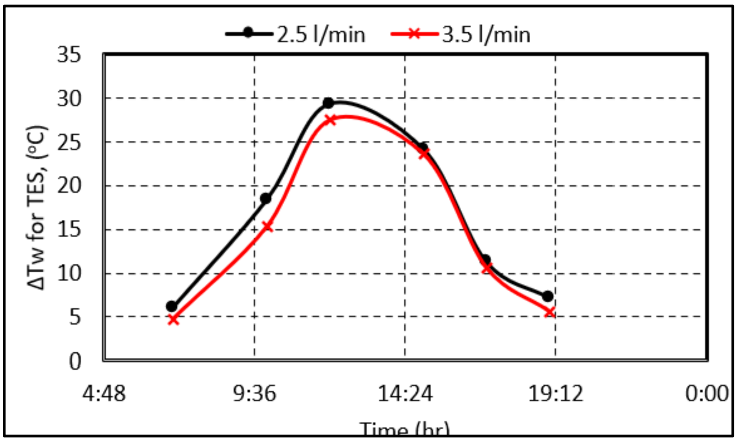


**Fig. 8. Simulated transient behaviour of the water temperature difference between the inlet and outlet for the TES system at different water flow rates.**

Figure 9 shows the instantaneous efficiency of the heating system for the FPMC model with the TES model at different water flow rates. The water working fluid at 2.5 l/min reached 50% efficiency at solar noon, and 34% efficiency was the least efficiency recorded at water working at 3.5%. The average overall efficiency for the water at 2.5 l/min was 57%, while the average overall efficiency was 49% with water working at 3.5 l/min. However, the rate of heat absorbed with water working at 2.5 l/min was higher than in the 3.5 l/min operation, and the heat loss rate was reduced.

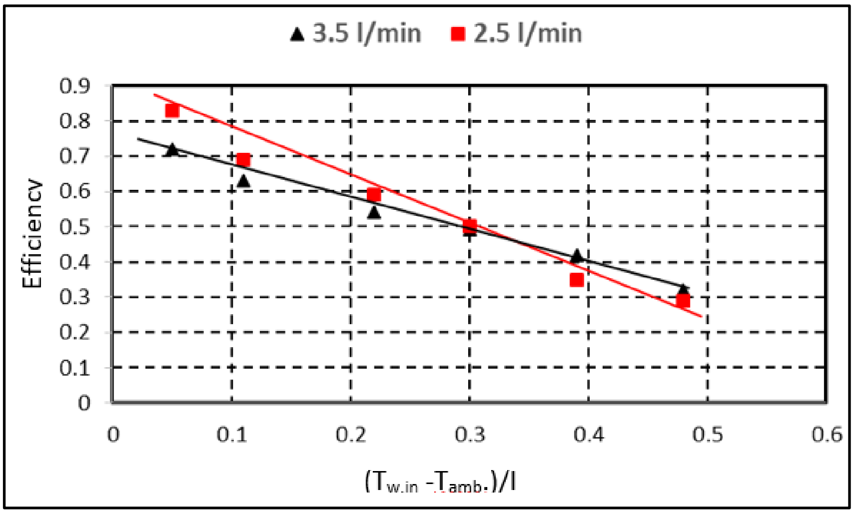


**Fig. 9. Instantaneous heating system efficiency for FPMC model with TES model at different water flow rates.**

## 4. Conclusions

This work describes a numerical analysis to study the influence of water flow rates through a heating system containing an FPMC unit and a TES unit. The temperature distribution for different water flow rates has been studied. The simulation was very carefully done to represent the physical situation closely. The following conclusions are drawn:

- For the FPMC model, Theoretical results showed that the difference in inlet and outlet temperatures decreases with increasing water flow rates, with the decreasing percentages being 11.5%, when changing the flow rate to 3.5 l /min.
- For the TES model, the net reduction of water heat to molten salts in the thermal energy storage unit has been chosen as the comparison parameter at the basic value at a low water flow rate of 2.5 l/min.
- For the close loop heating system, the average overall efficiency for the water at 2.5 l/min was 57%, while the average overall efficiency was 49% with water working at 3.5 l/min.

**Nomenclatures**

| | |
|---|---|
| $E$ | Total energy, J |
| $\vec{g}$ | Body acceleration, m/s$^2$ |

| | |
|---|---|
| $p$ | Pressure, N/m$^2$ |
| $T_{amb}$ | Ambient temperature, °C |
| $T_{w.in}$ | Inlet water temperature, °C |
| $\vec{V}$ | Flow velocity, m/s |
| ***Greek Symbols*** | |
| $\Delta T$ | Water temperature difference between the inlet and outlet of the cooling collector |
| $\rho$ | Density |
| **Abbreviations** | |
| CFD | Computational Fluid dynamics |
| PCM | Phase changing materials |
| FPMC | Flat porous media collector |
| TEC | Thermal energy storage |

## References


1. Abdul Wahhab, H.A.; and Al-Maliki, W.A.K. (2020). Application of a solar chimney power plant to electrical generation in covered agricultural fields. *IOP Conference Series, Material Science Engineering*, 671, 012137.
2. Al-Maliki, W.A.K.; Al-Hasnawi, A.G.T.; Abdul Wahhab, H.A.; Alobaid, F.; and Epple, B. (2020). A Comparison study on the improved operation strategy for a parabolic trough solar power plant in Spain. *Applied Sciences*, 11(20), 9576.
3. Abdul Wahhab, H.A.; Aljabair S.; and Ayed S.K. (2021). Assessment of wind fin performance run by mixed flows: experimental and numerical investigation. *Arabian Journal for Science and Engineering*, 46(12), 12077-12088.
4. Alesbe, I.; Abdul Wahhab H.A.; and Aljabair S. (2023). Transient study of thermal stratification of full-scale chilled water storage tank during optimum discharge condition. *Journal of Energy Storage*, 65, 107236.
5. Liu Z; (2015). *Global Energy Interconnection.* ISBN: 9780128044056, Elsevier Inc.
6. Kizilkan, O.; Kabul, A.; and Dincer, I. (2016). Development and performance assessment of a parabolic trough solar collector-based integrated system for an ice-cream factory. *Energy*, 100, 167-176.
7. Gude, V.G.; Nirmalakhandan, N.; Deng, S.; and Maganti, A. (2012). Low temperature desalination using solar collectors augmented by thermal energy storage. *Applied Energy*, 91(1), 466-474.
8. Conrado, L.S.; Rodriguez-Pulido, A.; and Calderón, G. (2017). Thermal performance of parabolic trough solar collectors. *Renewable and Sustainable Energy Rev*iew, 67, 1345-1359.
9. Colangelo, G.; Favale, E.; de Risi, A.; and Laforgia, D. (2013). A New solution for reduced sedimentation flat panel solar thermal collector using nanofluids. *Applied Energy*, 111, 80-93.
10. Fan, M.; Liang, H.; You, S.; Zhang, H., Zheng, W.; and Xia, J. (2018). Heat transfer analysis of a new volumetric based receiver for parabolic trough solar collector. *Energy*, 142, 920-931.

11. Younus, H.A.; Akroot, A.; Abdul Wahhab, H.A.; Talal, W.; Bdaiwi, M.; and Nawaf, M.Y. (2023). Impact of nano additives in heat exchangers with twisted tapes and rings to increase efficiency: A review. *Sustainability*, 15, 7867.
12. Xu, G.; Chen, W.; Deng, S.; Zhang, X.; and Zhao, S. (2015). Performance evaluation of a nanofluid- based direct absorption solar collector with parabolic trough concentrator. *Nanomaterials*, 5(4), 2131-2147.
13. Colangelo, G.; Favale, E.; Miglietta, P.; de Risi, A.; Milanese, M.; and Laforgia, D. (2015). Experimental test of an innovative high concentration nanofluid solar collector. *Applied Energy,* 154, 874-881.
14. Ajel, M.G.; Gedik, E.; Abdul Wahhab, H.A.; and Shallal, B.A. (2023). Performance analysis of an open-flow photovoltaic/thermal (PV/T) solar collector with using a different fins shapes. *Sustainability*, 15(5), 3877.
15. Ismaeel, A.A.; Abdul Wahhab, H. A.; and Naji, Z.H. (2021). Performance evaluation of updraft air tower power plant integrated with double skin solar air heater. *Evergreen*, 9, 678-688.
16. Al-Maliki, W.A.K.; Khafaji, H.Q.A.; Abdul Wahhab, H.A.; Al-Khafaji, H.M.H; Alobaid, F.; and Epple, B. (2022). Advances in process modelling and simulation of parabolic trough power plants: a review. *Energies*, 15(15), 5512.
17. Al-Maliki, W.A.K.; Abdul Wahhab, H.A.; Alobaid, F.; Epple, B.; and Abtan, A.A. (2023). Parabolic air collectors with an evacuated tube containing copper tube and spiral strip, and a new cavity receiver: experimental performance analysis. *Sustainability*, 15, 7926.
18. Khafaji, H.Q.A.; Abdul Wahhab, H.A.; Alsaedi, S.S.; Al-Maliki, W.A.K.; Alobaid, F.; and Epple, B. (2022). Thermal performance evaluation of a tubular heat exchanger fitted with combined basket–twisted tape inserts. *Applied Sciences*, 12(10), 4807.
19. Khafaji, H.Q.A.; Abdul Wahhab, H.A.; Al-Maliki, W.A.K.; Alobaid, F.; and Epple, B. (2022). Energy and exergy analysis for single slope passive solar still with different water depth located in Baghdad center. *Applied Sciences*, 12(17), 8561.
20. Basam, A. S.; Gedik; E.; Abdul Wahhab, H.A.; and Mohammed, G.A. (2020). Impact of Alumina nanoparticles additives on open-flow flat collector performance for PV panel thermal control application. *Evergreen*, 10(2).
21. Wang, F.; Shuai, Y.; Tan, H.; and Yu, C. (2013). Thermal performance analysis of porous media receiver with concentrated solar irradiation. *International Journal of Heat and Mass Transfer*, 62, 247-254.
22. Menbari, A.; Alemrajabi, A.A.; and Rezaei, A. (2017). Experimental investigation of thermal performance for direct absorption solar parabolic trough collector (DASPTC) based on binary nanofluids. *Experimental Thermal and Fluid Science*, 80, 218-227.
23. Dissa, A. O.; Ouoba, S.; Bathiebo, D.; and Koulidiati, J. (2016). A Study of a solar air collector with a mixed "porous" and "non-porous" composite absorber. *Solar Energy,* 129, 156-174.
24. Du, S.; Ren, Q.; and He, Y.L. (2017). Optical and radiative properties analysis and optimization study of the gradually varied volumetric solar receiver. *Applied Energy*, 207, 27-35.

25. Valizade, M.; Heyhat, M.M.; and Maerefat, M. (2019). Experimental comparison of optical properties of nanofluid and metal foam for using in direct absorption solar collectors. *Solar Energy Materials and Solar Cells*, 195, 71-80.
26. Mai; L.; Tian; X.; Xu; X.; Chang, L.; and Xu, L. (2014). Nanowire electrodes for electrochemical energy storage devices. *Chemical Reviews*, 114(23), 11828-11862.
27. Mehling; H.; Cabeza; L.F.; Hippeli, S.; and Hiebler, S. (2003). PCM-Module to improve hot water heat stores with stratification. *Renewable Energy*, 28(5), 699-711.
28. Dheep, G.R.; and Sreekumar, A. (2014). Influence of nanomaterials on properties of latent heat solar thermal energy storage materials-A review. *Energy Conversion and Management*, 83, 133-148.
29. Saw, C.L.; and Al-Kayiem, H.H. (2011). An investigation of integrated flat plate solar collector: experimental measurement. *National Postgraduate Conference*, (NPC2011), 19-20 September, Perak, Malaysia, IEEE Xplore, 1-6.
30. Al-Kayiem, H.H.; and Lin, S.C. (2014). Performance evaluation of a solar water heater integrated with a PCM nanocomposite TES at various inclinations. *Solar Energy*, 109(1), 82-92.
31. Benhouia, A.T.; Teggar, M.; and Benchatti, A. (2018). Effect of sand as thermal damper integrated in flat plate water solar thermal collector. *International Journal of Heat and Technology*, 36(1), 21-25.
32. Darwesh, B.D.; Hamakhan, I.A.; and Yaqob, B.N. (2022). Thermal enhancement of solar energy storage using phase change materials. *International Journal of Heat and Technology*, 40(3), 758-766.
33. Agalave, G.B.; Deshmukh, B.B.; and Kulkarni, P.R. (2013). Integration of solar flat plate collector and thermal energy storage for heating applications: an experimental study. *International Journal of Heat and Technology*, 41(5), 1335-1340.